DATA ON THE ππ INTERACTION DERIVED FROM PION PRODUCTION REACTIONS IN πp COLLISIONS

Ya. Ya. SHALAMOV and A. F. GRASHIN

Institute for Theoretical and Experimental Physics, Academy of Sciences, U.S.S.R.

Submitted to JETP editor November 22, 1961

J. Exptl. Theoret. Phys. (U.S.S.R.) **42**, 1115-1121 (April, 1962)

πp collisions of 2.8 BeV/c pions resulting in multiple production of pions were studied in a bubble chamber filled with a mixture of xenon and propane. In the reaction $\pi^- + p \to \pi^- + \pi^0 + p$ a strong interaction between the two final pions was observed. For the three pions with isospin I = 0 no interaction of the resonant character was observed. For all reactions the peculiarities in the energy and angular distributions are satisfactorily explained on the assumption that a significant contribution comes from the pole diagrams. The cross section for $\pi^-\pi^0$ scattering is $\sigma_{\pi\pi} \gtrsim 90$ mb at $\omega^2 = 20-30\,\mu^2$ and decreases rapidly with increasing pion energy.

IN a number of recently published papers [1-3] the processes $\pi N \to \pi\pi N$ were investigated for the purpose of obtaining information on the ππ interaction cross section. It was established that in the energy squared region of two pions $\omega^2 = 25-30\,\mu^2$ (μ is the pion mass) a resonant meson interaction with isospin I = 1 apparently exists. An analogous result was obtained using a 1.61 BeV/c antiproton beam (see [4]). In this work we study multiple pion production processes with the aim of obtaining information on the ππ interaction in a wider energy range.

1. EXPERIMENTAL SETUP

The multiple pion production on protons in the processes

$$\pi^- + p \to \pi^- + \pi^0 + p, \quad (1)$$
$$\pi^- + p \to \pi^- + \pi^0 + \pi^0 + p, \quad (2)$$
$$\pi^- + p \to \pi^- + \pi^- + \pi^+ + p, \quad (3)$$
$$\pi^- + p \to \pi^- + \pi^- + \pi^+ + \pi^0 + p. \quad (4)$$

was studied with the help of a 17 liter bubble chamber, filled with a mixture of xenon and propane (Xe —0.63 g/cm^3, C_3H_8 —0.33 g/cm^3).

The π^- mesons had a momentum of 2.8 ± 0.3 BeV/c. In the scanning of the stereophotographs approximately 170 two-prong and 120 four-prong stars were selected, in which one of the particles either stops in the chamber or has an ionization $J \geq 4-6$ times the minimum and can be identified by its range, ionization, and multiple scattering as a proton. Events for which the angle of inclination between the proton track and the plane of the photograph was $\varphi \geq 60°$ were not considered. The remaining prongs either are minimum ionizing or stop in the chamber and are identified as pions. In the case of two-prong stars it was required that one or more electron-positron conversion pairs, produced as a result of processes (1) or (2) with the subsequent decay of the neutral pions into photons, should be directed at the interaction point.

The events were analyzed with the help of a stereocomparator. The angles of emission and the ranges of the secondary charged particles were measured, as well as the angles of emission and the maximum possible path lengths in the chamber of photons. Selection of events occurring on free or weakly bound protons proceeded by standard methods based on the conservation laws. [5] In addition an estimate was made of the number of events due to protons bound in nuclei that can imitate hydrogen-like events: the photographic films were scanned when the working substance of the chamber was close to carbon (a mixture of two freons, whose combined chemical composition could be well described by the formula $C_2F_5Cl_3$) and when the chamber was filled with pure xenon. The momentum of the π^- mesons in these additional experiments was also 2.8 BeV/c.

The analysis of the events obtained from nuclei showed that the contribution from bound protons is small (about 20—30% for the various reactions), and that the form of the angular and energy distributions is close to the hydrogenic ones. The number of events of production of strange particles that could imitate reactions (1)—(4) was estimated. It turned out that corrections of this type are small

and they were not taken into account in the final results.

2. ANGULAR AND ENERGY DISTRIBUTIONS OF THE SECONDARY PARTICLES

The distribution of the events on free or weakly bound protons by the number of electron-positron pairs, directed at the interaction point, is as follows:

Reaction	No. of events
$\pi^- + p \to \pi^- + p + \gamma$	57
$\pi^- + p \to \pi^- + p + 2\gamma$	36
$\pi^- + p \to \pi^- + p + 3\gamma$	13
$\pi^- + p \to \pi^- + p + 4\gamma$	3
$\pi^- + p \to \pi^- + \pi^+ + \pi^- + p$	71
$\pi^- + p \to \pi^- + \pi^+ + \pi^- + p + \gamma$	14
$\pi^- + p \to \pi^- + \pi^+ + \pi^- + p + 2\gamma$	7
$\pi^- + p \to \pi^- + \pi^+ + \pi^- + p + 3\gamma$	1

Reactions (1) and (2), and also reactions (3) and (4), can be separated by using the known mean efficiency for registration of photons, calculated from the maximum possible path length of the given photon in the working substance of the chamber. The energy distribution of protons in the laboratory coordinate system (l.s.) for reactions (1), (2), and (3) is shown in Fig. 1a, b, and c, when the proton kinetic energy E_p is less than or equal to

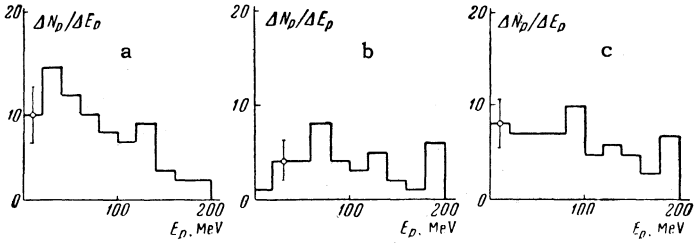

FIG. 1. Proton energy distribution in the l.s.: a—reaction (1), 71 events; b—reaction (2), 38 events; c—reaction (3), 65 events.

200 MeV. It may be noted that the forms of the spectra differ sharply from what one calculates in the statistical model of production. A second interesting peculiarity in the energy distributions consists of the fact that the average energy of the protons is less when two pions are produced than it is when three pions are produced.

Process (1) differs most sharply from processes (2) and (3) in the angular distributions of the protons in the l.s. (Fig. 2). For reaction (1) a sharply defined maximum is observed, and the half-width of the distribution decreases if the proton energy

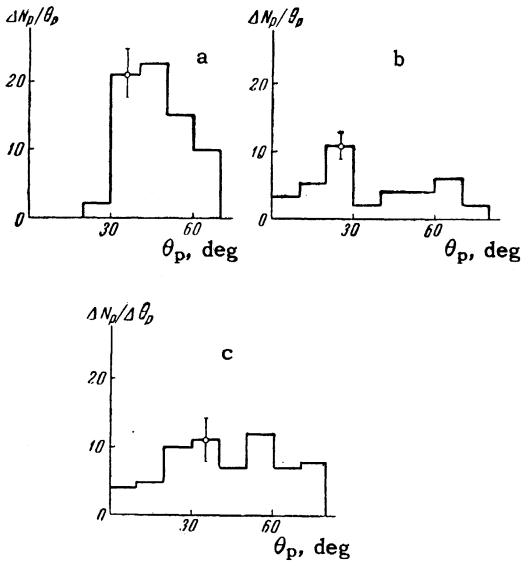

FIG. 2. Angular distribution of the protons in the l.s.: a—reaction (1); b—reaction (2); c—reaction (3).

is limited ($E_p \leq 100$ MeV). This fact is most naturally explained by the assumption that reaction (1) is a two-particle reaction as far as its kinematic parameters are concerned, with the peculiarities of the experimental method fixing reaction (1) when the proton energy lies between the limits 200 MeV $\gtrsim E_p \geq$ 10 MeV.

The angular distributions of the photons in the pion-nucleon center of mass system (c.m.s.), with the observation efficiency taken into account, are shown in Fig. 3a, b for reactions (1), (2). In the

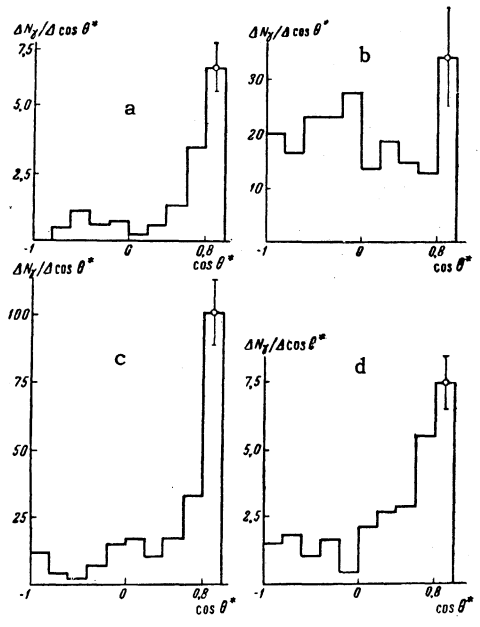

FIG. 3. Angular distribution of the photons in the c.m.s.: a—reaction (1), 83 photons; b—reaction (2), 90 photons; c—reaction (5), approximately 120 photons; d—reaction (6), approximately 100 photons.

discussion of the results it is convenient to have data on the angular distributions of photons produced in the processes

$$\pi^- + p \to \pi^0 + \pi^0 + n, \quad (5)$$
$$\pi^- + p \to \pi^0 + \pi^0 + \pi^0 + n. \quad (6)$$

The corresponding information was obtained from an analysis of the same photographic material [6] and is shown in Fig. 3c and d.

As can be seen from Fig. 3a and c the angular distribution of the photons in the c.m.s. is strongly peaked forward. This corresponds to the fact that the π^0 mesons produced in reactions (1) and (5) keep the direction of the incident π^- meson. The forward-backward ratio for the photons, with the observation efficiency taken into account, is $n = 4 \pm 1$ for reactions (1) and (5) and $n = 3.3 \pm 1$ for reaction (6). In the case of reaction (2) the photons in the c.m.s. are distributed isotropically ($n = 0.85 \pm 0.2$).

For reactions (1), (2), and (3) we have constructed the distributions of the number of events in ω^2, where ω is the total energy of the pions in their c.m.s. In Fig. 4a this distribution is shown for process (1) when the proton energy is $E_p \leq 100$ MeV. As can be seen from the figure, all 57 events are grouped near $\omega^2 \approx 35\,\mu^2$. In the case of reactions (2) and (3) the events are distributed uniformly throughout the energetically available interval of ω. The sum of the distributions for processes (2) and (3) is shown in Fig. 4b.

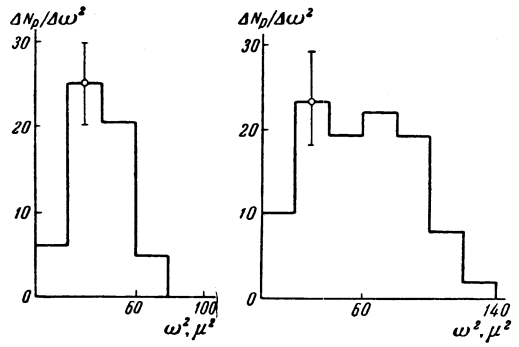

FIG. 4. Distribution of events in ω^2: a – reaction (1); b – sum of reactions (2) and (3).

3. TOTAL CROSS SECTIONS

In the determination of the cross sections for the processes (1)–(3) one runs into difficulties because of the need to have a precise estimate of the number of events due to quasi free protons in the nuclei of the working substance. Another significant uncertainty is due to the μ-mesonic contamination of the beam of the π^- mesons. In order to avoid these uncertainties we have calculated the total number of inelastic interactions and of events of the given type for a series of measurements with different working liquids. The cross section on hydrogen, calculated by the difference method, turned out for reaction (1) to be $\sigma = 2.3 \pm 0.4$ mb when $10 \leq E_p \leq 200$ MeV, and $\sigma = 1.8 \pm 0.4$ mb when $10 \leq E_p \leq 100$ MeV. The cross section for reaction (2) was $\sigma = 1.0 \pm 0.3$ mb when $10 \leq E_p \leq 200$ MeV.

4. THEORETICAL TREATMENT AND INTERPRETATION OF THE EXPERIMENTAL DATA

All experimentally detected properties of reactions (1)–(3), (5), and (6) are explained satisfactorily on the assumption that the pole diagrams provide a significant contribution to the cross section. Let us remark that from the theoretical point of view the conditions for the applicability of the pole approximation are more favorable in the case of reactions (2) and (6), since there the corresponding diagram (see, e.g., Fig. 5) contains the πN amplitude instead of the pseudoscalar vertex $g\gamma_5$ that appears in the analogous diagram for reactions (1) and (5).

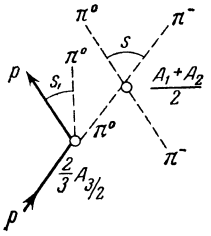

FIG. 5

The cross sections for reactions (1) and (5) are described in the pole approximation by the well known formula of Chew and Low [7] which in agreement with Fig. 1a gives a falling spectrum for the recoil nuclei $\sim 1/E$ (where E is the kinetic energy of the recoil nuclei in the l.s.). The distribution in the invariant $s = \omega^2$ in Fig. 4a indicates the resonant character of the cross section $\sigma_{\pi\pi}(s)$ for the process

$$\pi^- + \pi^0 \to \pi^- + \pi^0. \quad (7)$$

The cross section for reaction (7) calculated from the Chew-Low formula (integrated over the energy interval $10 \leq E_p \lesssim 100$ MeV) is shown in Fig. 6. In the region $\omega^2 > 25\,\mu^2$ the cross section falls rapidly; at $\omega^2 \approx 25\,\mu^2$ it amounts to $\sim 2/3$ the maximum possible for a partial P-wave amplitude ($I = 1$). This result is in agreement with the data

obtained in an analogous fashion with 1.89[2] and 1.4[3] BeV/c π^- mesons.

A more accurate description of reaction (1) may be obtained with the amplitude

$$\hat{A}(s, t) = A_p(s, t)\,\sigma\mathbf{p} - B\sigma\mathbf{p}_0, \qquad (8)$$

where $A_p(s,t)$ is the pole amplitude, $t = -2mE_p$ is the square of the momentum transfer, $\mathbf{p}_0$ and $\mathbf{p}$ are the momentum of the incident meson and proton in the l.s., σ is the Pauli matrix for the proton, m is the proton mass, and where the dependence on the invariants of the non-pole amplitude B may be ignored. The amplitude (8) corresponds to the cross section*

$$d^2\sigma(s, t)/ds\,dt = -t\,|A_p|^2 - \mathrm{Re}(A_p^* B)(s-\mu^2) + \{p_0^2\,|B|^2 + \mathrm{Re}(A_p^* B)\,t(\omega_0/m+1)\}, \qquad (9)$$

where $\omega_0 \approx p_0$ is the total energy of the incident meson. Let us call attention to the fact that the interference term in Eq. (9) gives rise to the same proton spectrum $\sim 1/E \sim 1/t$ as does the pole term, whereas the dependence of the remaining terms (in curly braces) on t may be ignored.

It is natural to assume that for $p_0 \approx 1.4$–2.8 BeV/c the last term in Eq. (9) is small, while the negative interference term amounts to at least $\frac{1}{3}$ of the pole term and therefore reduces the cross section given by the Chew-Low formula [first term in Eq. (9)]. An analogous negative, but stronger, interference is observed for $p_0 = 1$ BeV/c, as can be seen from the experimental curve for the cross section at $t = 0$ obtained by Anderson et al[1] [see Fig. 10 of [1] and its theoretical interpretation according to Eq. (9) of this paper]. Consequently, the more accurate analysis of the experimental data should result in a larger $\pi\pi$ cross section than that of Fig. 6 (and also larger than the cross sections obtained in [2,3]), while preserving the "resonant" shape of the curve. Agreement with the cross section of Anderson et al[1] ($\sigma_{\pi\pi} \approx 200$ mb at $s \approx 22\mu^2$) is obtained if it is assumed that in our case the interference term amounts to 50% of the pole term.

An analysis of reaction (5) according to the Chew-Low formula under the assumption of weak energy dependence of the invariant amplitude for the process $\pi^- + \pi^+ \to \pi^0 + \pi^0$ in the region $4\mu^2 \leq s \lesssim 2.5\,m^2$ leads to the following difference of scattering lengths in the states $I = 0$ and 2 (in units of $1/\mu$): $|a_0 - a_2| \approx 1$.

The cross section for reaction (2) corresponding to the diagram of Fig. 5 is of the form (see, e.g., [8])

$$d\sigma = \frac{\sigma(s_1)\sqrt{(s_1 - m^2 - \mu^2)^2 - 4m^2\mu^2}\,ds_1\,\sigma_{\pi\pi}(s)\sqrt{s(s-4\mu^2)}\,ds}{64\pi^3 m^2 p_0^2 (\tau - \mu^2)^2}\,d\tau, \qquad (10)$$

where $\sigma(s_1)$ is the cross section for the reaction $\pi^0 + p \to \pi^0 + p$ (s_1 is the square of the sum of the pion and nucleon energies in the c.m.s.), for which it is sufficient to consider only the contributions from the resonant 33 amplitude $A_{3/2}$, and τ is the square of the momentum transferred to the isobar $\pi^0 + p$. The minimum kinematically allowed value of $|\tau|$ in Eq. (10) is a function of s and s_1. For resonant values of s and s_1, which give the main contribution to the total cross section, $|\tau_{min}| \approx 6\mu^2$ which corresponds to a minimum proton energy $E_{p\,min} \approx 100$ MeV. Consequently the energy spectrum of the nucleons for reactions (2) and (3) should be shifted towards higher energies as compared with reaction (1) (compare Fig. 1a and Figs. 1b, c).

Substituting into Eq. (10) the cross section $\sigma_{\pi\pi}(s)$ from Fig. 6, integrating over the possible values of the invariants s_1, s, and τ and ignoring the interference between the peripheral and "isobaric" π^0 mesons,* we obtain for the cross section for reaction (2) approximately $\frac{1}{4}$ of its experimental value. It is natural to believe that the relative contribution of the pole diagram to reaction (2) should be, to say the least, larger than its contribution to reaction (1) (because of the presence of the amplitude $A_{3/2}$ instead of the pseudoscalar vertex $g\gamma_5$), and that the low value obtained is due to the use of too low a value for $\sigma_{\pi\pi}$. This

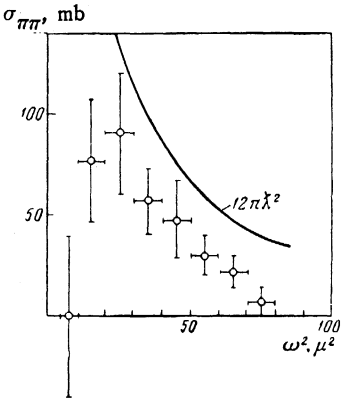

FIG. 6. Cross section for $\pi^-\pi^0$ scattering.

*The general expressions for the amplitude and cross section given in the second paper of Anderson et al[1] are incorrect: as compared with Eq. (8) the factor $\sigma \cdot p_0$ multiplying the non-pole amplitude is missing, which results in the absence in the cross section of the important interference term $\sim \mathrm{Re}(A_p^* B)$. The theoretical interpretation of Fig. 10 of[1] must be correspondingly altered.

*This reduces the contribution somewhat, but by no more than a factor of two.

provides additional evidence for the presence of the negative interference term in the cross section (9).

The pole approximation provides a simple explanation for the angular distribution of the photons. Indeed, for reactions (1) and (5) all the π^0 mesons are peripheral, i.e., are emitted forward in the c.m.s., giving rise to the corresponding distribution for the photons. For reaction (2), according to Fig. 5, the number of peripheral and "isobaric" π^0 mesons (which are emitted backwards in the c.m.s.) is the same, and consequently the forward-backward ratio for the photons is approximately equal to unity. For reaction (6) the pole diagram gives a foreard-backward ratio equal to two. The inclusion of non-pole diagrams, for which all three π^0 mesons are peripheral, increases this ratio. The experimental ratio of 3.3 may be obtained by assuming that the non-pole diagrams contribute approximately 30% of the experimental cross section.

The authors are grateful to A. I. Alikhanov, I. Yu. Kobzarev, and I. Ya. Pomeranchuk for discussion and useful remarks, and also to V. I. Smetanina and V. A. Kutilina for assistance in the work.

[1] Anderson, Bang, Burke, Carmony, and Schmitz, Phys. Rev. Lett. **6**, 365 (1961); Rev. Modern Phys. **33**, 431 (1961).

[2] Erwin, March, Walker, and West, Phys. Rev. Lett. **6**, 628 (1961).

[3] Pickup, Robinson, and Salant, Phys. Rev. Lett. **7**, 192 (1961).

[4] Maglić, Alvarez, Rosenfeld, and Stevenson, Phys. Rev. Lett. **7**, 178 (1961).

[5] N. G. Birger and Yu. A. Smorodin, JETP **37**, 1355 (1959), Soviet Phys. JETP **10**, 964 (1960).

[6] Ya. Ya. Shalamov and V. A. Shebanov, JETP **39**, 1232 (1960), Soviet Phys. JETP **12**, 859 (1961).

[7] G. F. Chew and F. E. Low, Phys. Rev. **113**, 1640 (1959).

[8] V. B. Berestetskiĭ and I. Ya. Pomeranchuk, JETP **39**, 1078 (1960), Soviet Phys. JETP **12**, 752 (1961).

Translated by A. M. Bincer
184